Journal of Power Sources 242 (2013) 699–713

Contents lists available at SciVerse ScienceDirect

Journal of Power Sources

journal homepage: www.elsevier.com/locate/jpowsour

Adaptive state of charge estimator for lithium-ion cells series battery pack in electric vehicles

Rui Xiong [a,b,*], Fengchun Sun [a], Xianzhi Gong [b], Hongwen He [a]

[a] National Engineering Laboratory for Electric Vehicles, School of Mechanical Engineering, Beijing Institute of Technology, No. 5 South Zhongguancun Street, Haidian District, Beijing 100081, China
[b] DOE GATE Center for Electric Drive Transportation, Department of Electrical and Computer Engineering, University of Michigan, Dearborn, MI 48128, USA

HIGHLIGHTS

- A bidirectional resistor based lumped parameter equivalent circuit model is proposed.
- Cells imbalanced parameters are analyzed and used for cells filtering approach.
- Cells filtering approach for ensuring voltage/SoC balancing is proposed.
- Cells series connected battery pack model is built and evaluated by cell unit model.
- Battery pack's SoC is accurately estimated by AEKF-based method with unit model.

ARTICLE INFO

Article history:
Received 27 February 2013
Received in revised form
15 May 2013
Accepted 17 May 2013
Available online 28 May 2013

Keywords:
Electric vehicles
Battery pack
Adaptive extended Kalman filter
State of Charge
Filtering
Unit model

ABSTRACT

Due to cell-to-cell variations in battery pack, it is hard to model the behavior of the battery pack accurately; as a result, accurate State of Charge (SoC) estimation of battery pack remains very challenging and problematic. This paper tries to put effort on estimating the SoC of cells series lithium-ion battery pack for electric vehicles with adaptive data-driven based SoC estimator. First, a lumped parameter equivalent circuit model is developed. Second, to avoid the drawbacks of cell-to-cell variations in battery pack, a filtering approach for ensuring the performance of capacity/resistance conformity in battery pack has been proposed. The multi-cells "pack model" can be simplified by the unit model. Third, the adaptive extended Kalman filter algorithm has been used to achieve accurate SoC estimates for battery packs. Last, to analyze the robustness and the reliability of the proposed approach for cells and battery pack, the federal urban driving schedule and dynamic stress test have been conducted respectively. The results indicate that the proposed approach not only ensures higher voltage and SoC estimation accuracy for cells, but also achieves desirable prediction precision for battery pack, both the pack's voltage and SoC estimation error are less than 2%.

1. Introduction

Energy crises, environmental issues and concerns regarding peaking oil production have promoted research into development of various types of electric vehicles (EVs), which has been established as one of the seven strategic emerging industries in China. In recent years, lithium-ion batteries have attracted special attention for EVs applications because of the high power density, high energy density and long lifetime [1,2]. In order to satisfy the operation voltage and traction power requirements of various EVs, low voltage lithium-ion cells are generally connected in series, parallel or series/parallels to construct a stable lithium-ion battery pack. In such applications, a battery management system (BMS) is critical for maintaining optimum battery performance and ensuring safety in EVs. The most important key function of the BMS is to monitor the State of Charge (SoC) from a model-based estimation algorithm for the cells strung lithium-ion battery pack [3–6]. Accurate SoC estimates improve the power distribution efficiency and extend the batteries' expected life greatly. Unfortunately, due to cell-to-cell variations in the battery pack, it is hard to model the battery pack accurately. As a result, accurate SoC estimation for battery pack remains very challenging and problematic.

* Corresponding author. National Engineering Laboratory for Electric Vehicles, School of Mechanical Engineering, Beijing Institute of Technology, No. 5 South Zhongguancun Street, Haidian District, Beijing 100081, China. Tel./fax: +86 10 6891 4842.
E-mail addresses: rxiong6@gmail.com, rxiong@umich.edu (R. Xiong).

0378-7753/$ – see front matter © 2013 Elsevier B.V. All rights reserved.
http://dx.doi.org/10.1016/j.jpowsour.2013.05.071

An assortment of techniques has previously been reported to measure or estimate the SoC of the cells or battery packs, each having its relative merits, as reviewed by Xiong et al. [7]. The most common method is the ampere-hour (Ah) integral/counting method, which is based on both current measurement and integration [8]. However, its performance is highly dependent on the measuring accuracy of current, and this open-loop calculation method can easily lead to accumulated calculation errors due to uncertain disturbances from the practice application and lack of necessary corrective resolution. Therefore, the method that is often recalibrated by the equilibrium open circuit voltage (OCV) method [6], the support vector based estimators [9], the artificial neural networks (ANNs) and fuzzy logic principle based estimations [10,11], sliding mode observer [12], the extended Kalman filtering (EKF) based estimators [13–17] and others [18,19]. Most of the methods have been widely used and made acceptable achievements in different applications.

A common drawback of the above methods for the battery packs is that the difference between each individual battery cell has been ignored and the work mainly focuses on estimating the SoC for a battery "cell". As we know, for the vehicular operation, due to the voltage and power/energy requirements, the battery systems are usually composed of up to hundreds of cells connected in series or parallel. The battery system has less available capacity when the cells in the battery pack are not balanced. Specifically, the weakest cell limits the discharge capacity of an imbalanced battery pack. During the discharge and charge operation, the weakest cell will reach the minimum discharge level and the maximum charge level before the rest of the cells [20,21]. As a result, this parameter variation among the cells makes "pack model" and "pack state" values hardly providing sufficient information, which at last affects the prediction precision of available energy and power and even damages the battery systems.

So for a reliable and accurate battery management, the BMS should calculate each individual cell's state and use the lowest SoC to avoid the over-discharge and use the highest SoC to avoid the over-charge condition. One possible solution is to design an estimator which works well for estimating single cell SoC, and to replicate the estimator N times to estimate all SoCs for the N cells in a battery pack [22]. However, due to limited computing ability of an automotive embedded system, it is hard to implement online calculations for N cells. Kim et al. [17] proposed a method to improve SoC estimation of a lithium-ion battery pack based on a screening process, which in some degree guarantees the uniformity of the cells, and makes it possible to be used in BMS. One of the limitations of the method is that, in actual operation, the method will reduce the acceptance proportion of tested cells, most of the cells have been eliminated, only two or three of twenty have been chosen. Another limitation is the variance threshold of the cells is not discussed, which is very important for improving the acceptance proportion. Last is the EKF-based SoC estimator is vulnerable to divergence from imbalanced cells behavior. Dai et al. [20] introduced a dual time-scale EKF based cells SoC estimation method with an "averaged cell" model. The result indicates the good performance of the algorithm. However, one of the limitations of the method is that, in actual using, the computation cost is higher. More importantly, there are some problems required to be solved before the dual-EKF applied to practical application. Roscher et al. [21] introduced a reliable state estimation of multi-cell lithium-ion battery systems, by which cell impedance and SoC variations could be detected precisely. However, the detailed process of how to determine the tunable correction gain was not discussed in the paper. In additional, this work also requires a prohibitive level of computation for battery systems. Plett [22] explored a cute method called "bar-delta filtering" which took advantage of the fundamental similarity between all series connected cells in a pack and could estimate SoC, resistance and capacity of each cell in a manner requiring only somewhat more computational effort than that for a single cell. Aiming at SoC estimation for lithium-ion battery pack of multi-cells in series, Liu et al. [23] proposed a minimal cell load voltage (V_{min}) of the battery pack based SoC estimation method. With EKF algorithm, the dynamic state estimation of SoC is realized. However, V_{min} model-based method ignored the problem of overcharge from the cell with maximum terminal voltage. Another limitation is "V_{min}" cell not always the cell with lowest capacity in the battery pack; as a result, the SoC prediction error will be larger in this situation.

In this study, aiming at reliable and accurate SoC estimation for lithium-ion battery pack of multi-cells in series, on one hand, based on the lumped parameter equivalent circuit model, the unit model is proposed and used for estimating the terminal voltage and state for cells having similar electrochemical characteristics: similar capacity, resistance and other characteristics. The unit model is also employed for estimating the battery pack's voltage and state; on the other hand, a systematic cells filtering approach is proposed for choosing cells with similar electrochemical characteristics, afterward the chosen cells are assembled to a series connected battery pack. Through the filtering process, the cells that have similar electrochemical characteristics are finally chosen, and each cell can be used as a unit model. This approach has the potential to eliminate the drawbacks of cell-to-cell variations and reduce the influence of EVs from the imbalanced battery cells and packs. As a result, the performance of the battery pack which has good capacity/resistance conformity can be described with a cell unit model. At last, we can use the unit model to estimate the state of the battery system. However, the filtering threshold is crux for improving the choosing intensity of the tested cells. Additionally, the adaptive extended Kalman filter (AEKF), which can improve the prediction precision by adaptively updating the process and measurement noise covariance, is applied to estimate the battery pack's SoC with the cell unit model.

The remainder of the paper is organized as follows. Section 2 shows the main imbalanced parameters of cells and the basic concept of the filtering approach, which is used for filtering the cells having similar electrochemical characteristics, and at last a detail flowchart for filtering approach is presented. In Section 3, a cells series connected battery pack model is build based on the cell lumped parameter equivalent circuit unit model and then the AEKF-based SoC estimator is proposed for estimating the state of battery pack through the unit model. Section 4 describes the cells test, as a case, a total of 20 lithium-ion polymer battery (LiPB) cells are used for carrying out the cells filtering process. Section 5 evaluates the estimation accuracy of AEKF-based battery SoC estimator for estimating the battery pack's terminal voltage and SoC. Specifically, in order to compare the SoC estimation accuracy for chosen cells series connected battery pack and the other cells series connected battery pack and to evaluate the filtering approach, the dynamic stress test-based comparative simulations are conducted and the estimation results suggest that the proposed approach is reliable. In the final section, some conclusions and final remarks are given.

2. Cells filtering approach

2.1. Cells inconsistent characteristic parameters

In general, the more numbers of the cells connected in battery systems, the greater of the difference exist in cells parameters. What's worse, the differences in cells' performance caused by the manufacturing chain coupling with the operation conditions of the

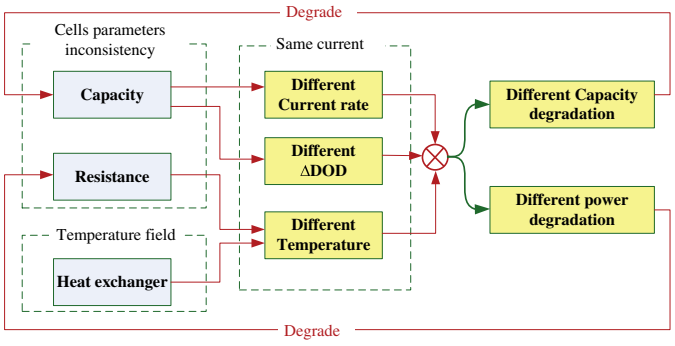

Fig. 1. Main factors causing battery performance degradation.

battery system will lead to different degradation rate in their performance, which in turn spread the differences in individual cells.

Generally speaking, it is difficult to fully guarantee the conformity of the initial performance parameters as well as the intrinsic or extrinsic operation conditions of battery systems, and this unconformity leads to a difference in battery state. As a result, the difference in battery performance degradation is aggravated by the difference in battery state in turn. Both mutual coupling effects are shown in Fig. 1.

The research on battery calendar-life indicates that the main factors, which degrade the battery performance, are different current rates, different depths of the discharge (ΔDOD) and different operation temperatures [24,25]. For the cells in battery packs, even if the same operating currents, the actual discharge and charge current rates and DOD are different since the difference in cells capacity. On the other hand, due to the difference in cells resistance, the heat exchanger for each individual cell is different, without an efficient and proper design for temperature field, the actual intrinsic or extrinsic operation temperatures are quite different. Additionally, for a parallel connected battery pack, the difference in cells resistance and connection resistor will lead to a difference in discharge and charge currents too. The above factors in the practical battery operation process are coupling together, and eventually lead to different degradation rate for individual cells in battery pack. And those differences exacerbate the imbalance in cells capacity, resistance etc. As a result, these form a positive feedback effect.

2.2. Cells filtering approach

The purpose of this paper is to present a new approach based on a filtering approach for improved capacity/resistance balancing of a lithium-ion series battery pack. The approach has the potential to overcome the drawbacks of cell-to-cell variations and achieve a good voltage/SoC balancing for battery pack. The filtering process is for choosing the cells that have similar capacity and resistance. Two steps of filtering process, such as capacity filtering and resistance filtering, are implemented in an orderly manner, as shown in Fig. 2.

After the filtering process, the cells with similar electrochemical characteristics have been chosen and then ready for packing. The cells and battery pack are kept in the thermal chamber and their temperatures are controlled within constant values, therefore the heat exchanger is not discussed in this filtering process. The detailed filtering process is described as follows.

2.2.1. Capacity filtering process

The available capacity test, which is on the basis of the standard of Ref. [26], is performed to measure the cells' maximum available capacity. The maximum available capacity C_n of the cell is the number of ampere-hours that can be drawn from the battery at the nominal current (½C rate), starting with the battery fully charged, which is maybe different with its nominal value due to the operation environment and aging levels. Usually, the available capacity test is repeated three times. If the error of the experiment results between the peak and the average is within 2%, the available capacity test is effective and the average value is taken as the actual maximum available capacity. However, if the error is more than 2%, the available capacity test should be repeated and ends by achieving three continuous effective tests.

To achieve an accurate SoC estimates with the error less than ±5%, the cells capacity variance should be controlled within ±5% ranges deviating from the average capacity of tested cells. It is noted that, with an efficient model-based SoC estimation approach, the SoC prediction error can be reduced to less than 5% through a robust closed-loop corrections from cell parameters even if its capacity error more than 5%.

2.2.2. Resistance filtering process

After the first filtering process, the chosen cells are required to carry out the resistance filtering process. Two parts, fast voltage transients and slower voltage variances caught by the discharge and charge pulse current. Fig. 3 shows the discharge and charge pulse current and terminal voltage profile at a specified SoC of HPPC (hybrid power pulse characteristic) test [27]. For simplicity, the voltage resistance can be calculated by their voltage variance. The

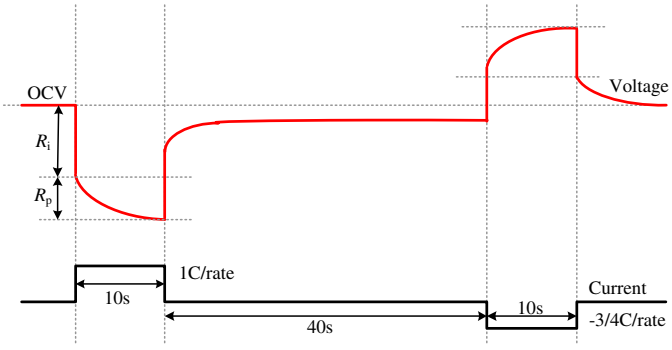

Fig. 3. Discharging and charging pulse current and voltage profile from HPPC test.

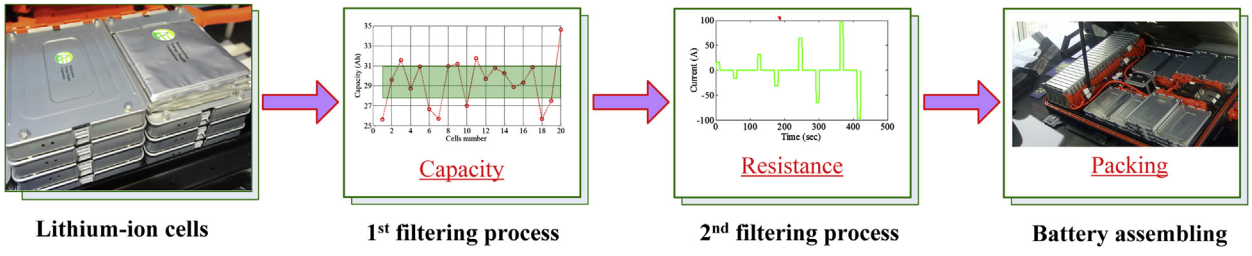

Fig. 2. An implementation flowchart of the cells filtering approach.

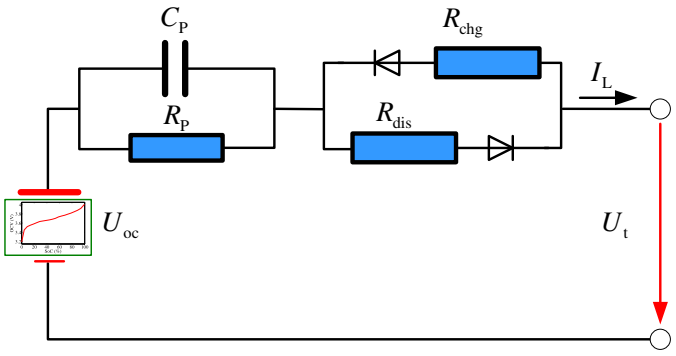

Fig. 4. Schematic diagram for lumped parameter equivalent circuit model.

dynamics of the cell can be described as lumped parameter equivalent circuit model that is comprised of OCV part-U_{oc}, a resistor R_i includes R_{dis} at discharge and R_{chg} at charge, and an RC network connected in series, which is shown in Fig. 4. Fig. 3 shows the fast voltage transients. Those associated with the electrical resistance of various cell components or with the accumulation and dissipation of charge in the electrical double layer, are assigned to the resistor in the circuit model, and the slower voltage transients arising from mass transport effects are assigned to the RC component. The elements of that component are accordingly described as the diffusion resistance R_P and diffusion capacitance C_P.Where I_L is the load current (assumed positive for discharge, negative for charge) and U_t is the terminal voltage.

The accuracy of the second filtering process depends largely on the model parameters' values used in the lumped parameter model of the battery system. As shown in Fig. 4, it is very important to correctly calculate the resistor R_i and diffusion resistance R_P for resistance filtering process. To get more appropriate parameters, we use four groups of current profiles to excite the cells and calculated the parameters. To reduce the imbalance behavior of cells voltage, we set the inconsistency threshold of resistor R_i based on their average resistance, and with this threshold the cells voltage variance from the inconsistent resistance may be reduced to 1% of their nominal voltage. Noted that we can decrease the threshold to achieve much less variance of cells' terminal voltage, but it reduces the numbers of the chosen cells and increases the cost of the battery system. Therefore, we try to put the emphasis on maximizing the chosen amount of the tested cells and minimizing the control error. However, the battery pack's terminal voltage estimation error which is caught by the inconsistent cells' parameters will be reduced and converge to the cells with or close to average cell parameters by the compensating from their selves, which beneficial to the pack's prediction precision.

Based on the above analysis, we can conclude the detail step for filtering process and shown in Fig. 5.

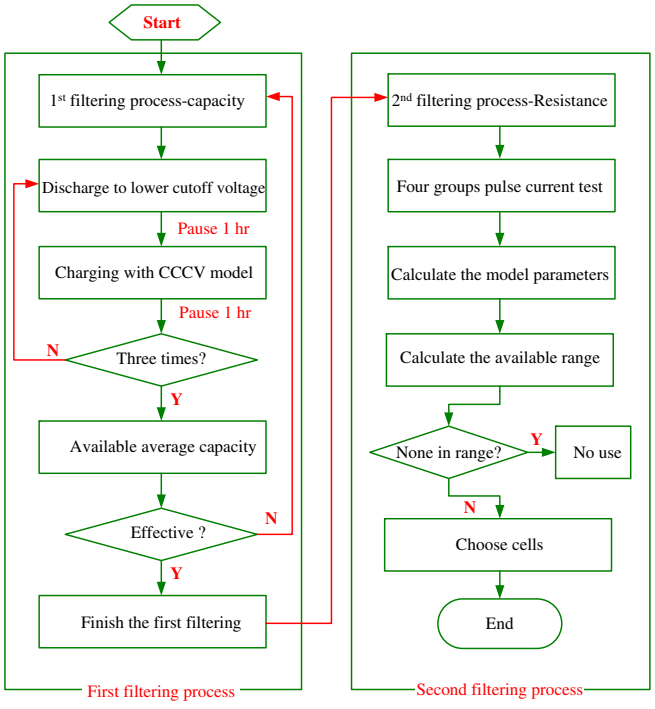

Fig. 5. Detail operation procedure of cells filtering approach.

3. Adaptive SoC estimator for battery pack

3.1. Modeling technique

3.1.1. Cell unit model

To achieve a reliable battery state estimation, an accurate model must be built first. The schematic diagram for lumped parameter equivalent circuit model is shown in Fig. 4. To improve the model's prediction precision further, we try to find a better OCV function to improve its simulation accuracy and make SoC available as part of the model state. The electrical behavior of the proposed model can be expressed by Eq. (1).

$$\begin{cases} \dot{U}_P = -\dfrac{1}{C_P R_P} U_P + \dfrac{1}{C_P} I_L \\ U_t = U_{oc} - U_P - U_R \end{cases} \tag{1}$$

where U_P is the voltage across C_P. U_R is the fast transient voltage from resistor R_i, therefore:

$$U_R = \begin{cases} I_L \times R_{dis} & (\text{discharge}) \\ -I_L \times R_{chg} & (\text{charge}) \end{cases} \tag{2}$$

The open circuit voltage U_{oc} is described by Eq. (3).

$$U_{oc} = K_0 + K_1 z + K_2 z^2 + K_3 z^3 + K_4/z + K_5 \ln(z) \tag{3}$$

where z is the abbreviation of SoC, K_i $(i = 0, 1, \ldots 5)$ are six constants which uses to fit the SoC vs. OCV data well.

3.1.2. Modeling for battery pack

With the proposed filtering process, the cells with similar performance have been chosen finally. As a result, the lumped parameter battery model, which comprises ***N*** cells, can be simplified as a cell unit model. Consequently, as shown in Fig. 6, the series connection of cell unit model for NS1P (***N*** series and **1** parallel) battery pack that reflects the series battery pack is equivalent to a

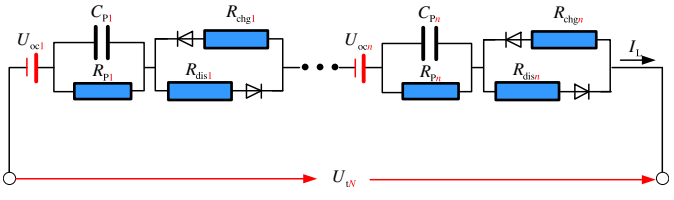

Fig. 6. Series connection of cell lumped parameter model unit model for NS1P battery pack.

series connection of cell unit models. Then, based on the filtering results, this lumped parameter pack model can be simplified as that of the unit model, as shown in Fig. 7. Therefore, in this overall perspective, the relation between the cell unit and N cells series battery pack can be calculated as follows.

$$U_{ocN} = U_{oc1} + U_{oc2} + \ldots U_{ocn} = \sum_{i=1}^{n} U_{oci} = NU_{oc} \quad (4)$$

$$R_{disN} = R_{dis1} + R_{dis2} + \ldots R_{disn} = \sum_{i=1}^{n} R_{disi} = NR_{dis} \quad (5)$$

$$R_{chgN} = R_{chg1} + R_{chg2} + \ldots R_{chgn} = \sum_{i=1}^{n} R_{chgi} = NR_{chg} \quad (6)$$

$$R_{PN} = R_{P1} + R_{P2} + \ldots R_{Pn} = \sum_{i=1}^{n} R_{Pi} = NR_{P} \quad (7)$$

$$C_{PN} = C_{P1} = C_{P2} = \ldots C_{Pn} = C_{Pi} = C_{P} \quad (8)$$

$$U_{tN} = U_{ocN} - U_{PN} - U_{RN} = \sum_{i=1}^{n} R_{chgi} U_{ti} = NU_{t} \quad (9)$$

where the U_{ocN} is the OCV of the battery pack, and the U_{oci} is the OCV of cell i (i = 1,2,……,n). R_{disN} and R_{chgN} are the discharge and charge resistances of the battery pack respectively. The R_{disi} and R_{chgi} are the discharge and charge resistance of the cell i respectively. R_{PN} is the diffusion resistance of the battery pack, and the R_{Pi} is the diffusion resistance of cell i, C_{PN} is the diffusion capacitance of the battery pack, and the C_{Pi} is the diffusion capacitance of cell i. The U_{tN} is the terminal voltage of the battery pack, and U_{ti} is the terminal voltage of cell i.

According to the number of cells in series (N), the terminal voltage of the simplified lumped parameters model is properly determined by:

$$NU_{t} = N(U_{oc} - U_{P} - U_{R}) \quad (10)$$

3.2. Adaptive extended Kalman filter-based SoC estimator

3.2.1. Review of adaptive extended Kalman filter

The Kalman filter is a mathematical technique that provides an efficient recursive means for estimating the states of a process, in such a way so as to minimize the mean of the squared error. In order to use EKF for state estimation, we must first have a system model in a state-space form [7]. Specifically, we assume a very general framework for discrete-time lumped dynamic systems.

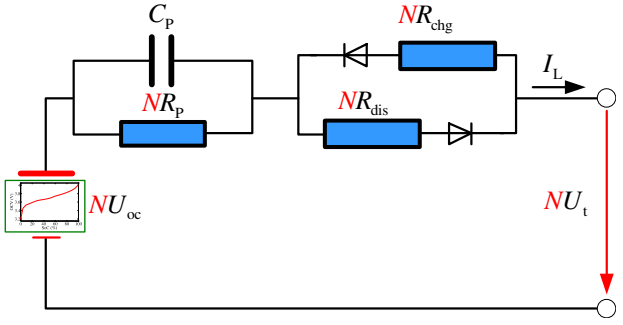

Fig. 7. Simplified lumped parameters model for NS1P battery pack.

$$\mathbf{X}_{k+1} = \mathbf{A}\mathbf{X}_k + \mathbf{B}\mathbf{u}_k + \omega_k \quad (11)$$

$$\mathbf{Y}_{k+1} = \mathbf{C}\mathbf{X}_{k+1} + \mathbf{D}\mathbf{u}_k + \upsilon_k \quad (12)$$

where $\mathbf{X}_k$ is the system state vector at the kth sampling interval, which represents the total effect of system inputs $\mathbf{u}_k$ on the present system operation, such as SoC. ω_k is the unmeasured "process noise" that affects the system state and υ_k is the measurement noise which does not affect the system state, but can be reflected in the system output estimates $\mathbf{Y}_k$. And ω_k is assumed to be Gaussian white noise with zero mean and covariance $\mathbf{Q}_k$; υ_k is assumed to be Gaussian white noise with zero mean and covariance $\mathbf{R}_k$. The matrices $\mathbf{A}$, $\mathbf{B}$, $\mathbf{C}$ and $\mathbf{D}$ describe the dynamics of the system.

A drawback of the Kalman filter is the dependence on a good estimation of $\mathbf{Q}$ and $\mathbf{R}$. A Kalman filter basically assumes that the covariance of both the process and the measurement noise are known. Thus, in practice, inappropriate initial noise information will make the approach fail to ensure its performance. Otherwise, the covariance values can be estimated to improve the performance of the Kalman filter by employing an AEKF approach. The AEKF provides a further innovation in the algorithm using the filter's innovation sequence. The innovation allows the parameters $\mathbf{Q}_k$ and $\mathbf{R}_k$ to be estimated and updated iteratively from the following equations [14]:

$$\mathbf{H}_k = \frac{1}{M} \sum_{i=k-M+1}^{k} \mathbf{e}_i \mathbf{e}_i^T \quad (13)$$

$$\begin{cases} \mathbf{Q}_k = \mathbf{K}_k \mathbf{H}_k \mathbf{K}_k \\ \mathbf{R}_k = \mathbf{H}_k - \mathbf{C}_k \mathbf{P}_k^- \mathbf{C}_k^T \end{cases} \quad (14)$$

where $\mathbf{H}_k$ is the innovation covariance matrix based on the innovation sequence $\mathbf{e}_i$ inside a moving estimation window of size M.

An implementation flowchart of the AEKF algorithm is listed in Fig. 8 for a parameter identification or state estimation.

3.2.2. State of Charge definition

The SoC is defined as the available capacity expressed as a percentage of maximum available capacity, and it is given by:

$$z_k = z_0 - \frac{1}{C_n} \int_0^k \eta_i I_{L,\tau} d\tau \quad (15)$$

where z_k is the SoC at kth sampling intervals, z_0 is the initial SoC, $I_{L,\tau}$ is the instantaneous load current; η_i is the coulomb efficiency, which is the function of the current and the temperature; C_n is the present maximum available capacity.

Describing Eq. (15) with a discrete-time form, we can get:

$$z_k = z_{k-1} - \eta_i I_{L,k} \Delta t / C_n \quad (16)$$

where Δt is the sampling interval (in hours). Eq. (16) is the basis to calculate the SoC as the state and current $I_{L,k}$ at the kth sample time as the input in the state vector of the battery model as it is in state equation format.

3.2.3. SoC estimator for battery pack

Transform the Eq. (1) to a discrete format:

$$\begin{cases} U_{P,k} = U_{P,k-1}\exp(-\Delta t/(\tau)) + I_{L,k-1}R_P(1-\exp(-\Delta t/\tau)) \\ U_{t,k} = U_{oc}(SoC_k) - I_{L,k}R_o - U_{P,k} \end{cases} \tag{17}$$

The state equation and observation equation of the discrete system of interest is as follows.

$$\begin{aligned} \mathbf{x}_k &= \begin{pmatrix} U_{P,k} \\ SoC_k \end{pmatrix}, \quad \mathbf{A}_k = \begin{pmatrix} \exp(-\Delta t/(R_PC_P)) & 0 \\ 0 & 1 \end{pmatrix}, \\ \mathbf{B}_k &= \begin{pmatrix} R_P(1-\exp(-\Delta t/(R_PC_P))) \\ \eta_i \Delta t/C_n \end{pmatrix} \\ \mathbf{C}_k &= \left.\frac{\partial U_t}{\partial \mathbf{x}}\right|_{\mathbf{x}=\widehat{\mathbf{x}}_k^-} = \left[-1 \quad \left.\frac{dU_{oc}(SoC)}{dSoC}\right|_{SoC_k^-}\right], \quad \mathbf{D}_k = [R_i], \end{aligned} \tag{18}$$

where the calculation of $dU_{oc}(SoC)/dSoC$ is calculated as follows:

$$\frac{dU_{oc}(SoC)}{dSoC} = K_1 + 2K_2z + 3K_3z^2 - K_4/z^2 + K_5/z \tag{19}$$

The discharge and charge current is loaded on the lithium-ion cell and the unit model simultaneously. Terminal voltage error between the estimation and the experimental data is reduced by adaptively updating the AEKF observer gain. Then the observer with the updated gain is used to compensate for the state estimation error. The estimation of SoC is then fed back to update the parameters of the battery model for the next SoC estimation. And the SoC estimation method based on AEKF is shown in Fig. 9.

With the terminal voltage and SoC estimator based on the cell unit model and filtering approach, the state of the battery pack can be estimated.

4. Application to LiPB cells

4.1. Battery experiment

4.1.1. Experiment setup

The test bench setup is shown in Fig. 10. It consists of a battery testing system (Arbin BT2000), a thermal chamber for environment control, a computer for the human–machine interface and experimental data storage and the cells or battery pack. The battery testing system is responsible for loading the battery cells/module based on the customer's program with a highest voltage of 60 V and maximum charging/discharging current of ±300 A with three scales (5 A/50 A/300 A). The host computer is used to control the Arbin BT2000 and thermal chamber, and record many quantities, such as load current, terminal voltage, Amp-hours (Ah) and Watt-hours (Wh). The cell voltage can also be measured by the auxiliary channel, and its measuring range is 0–5 V. The measurement inaccuracy of the current transducer inside the Arbin BT2000 system is within 0.1%. The measured data is transmitted to the host computer through TCP/IP ports. The Arbin BT2000 is connected to the battery cells/module, which is placed inside the thermal chamber to maintain the temperature. The temperature operation range of the thermal chamber is between −55 °C and 85 °C.

4.1.2. Test schedule

The test schedule for our research is shown in Fig. 11, which is designed to collect the cells/packs test data under our designed

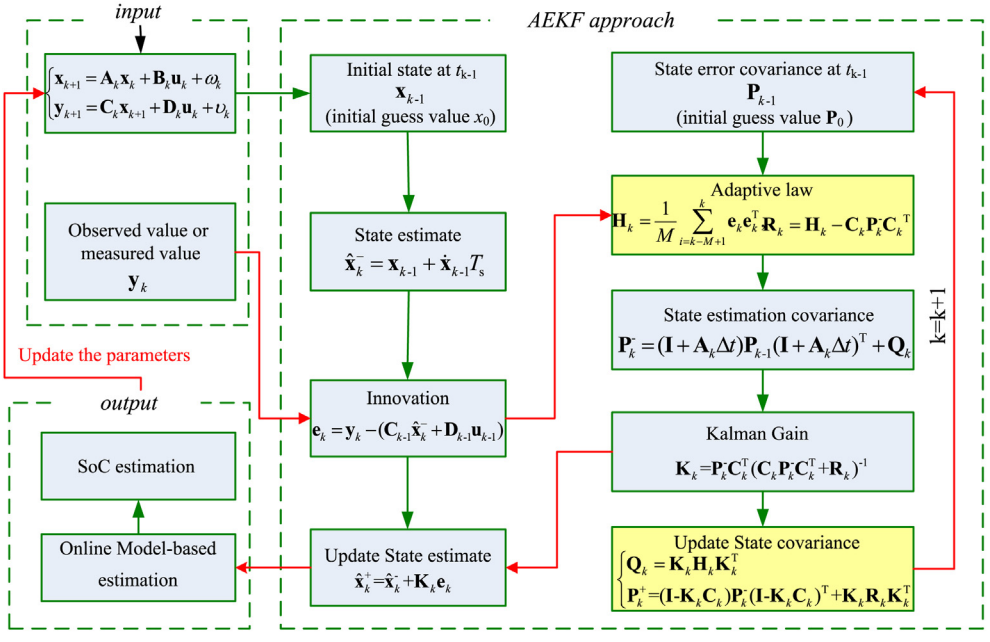

Note:Where $\mathbf{K}_k$ is the kalman gain matrix; $\mathbf{e}_k$ is defined as the difference between the measurement and the observation $\mathbf{C}_{k-1}\hat{\mathbf{x}}_k^- + \mathbf{D}_{k-1}\mathbf{u}_{k-1}$, $\hat{\mathbf{x}}_k^+$ and $\hat{\mathbf{x}}_k^-$ are for the *priori* estimate *before* the measurement is taken into account and the *posteriori* estimate after the measurement is taken into account respectively.t_{k-1} is the initial time of calculation.

Fig. 8. An implementation flowchart of the AEKF algorithm.

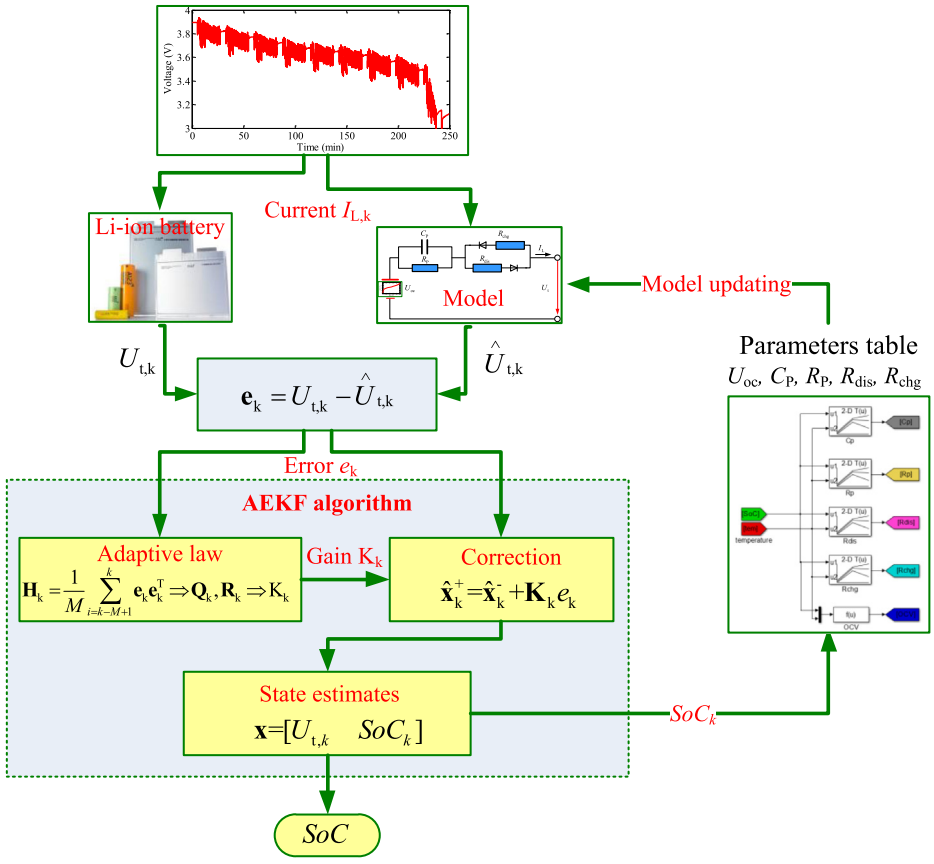

Fig. 9. An implementation flowchart of the data driven-based SoC estimation approach.

program. The datasheets and the test method for characteristic test are described in details in Ref. [14]. The federal urban driving schedule (FUDS) loading profiles are used to verify and evaluate the robustness of the state estimator with unit model, and the dynamic stress test (DST) loading profiles are used to verify and evaluate the performance of the adaptive SoC estimator for series connected battery pack. The datasheet with the battery operating temperature of 25 °C is used in the paper.

A total of 20 LiPB cells were used for our research. In the maximum available capacity test, we find that the biggest capacity

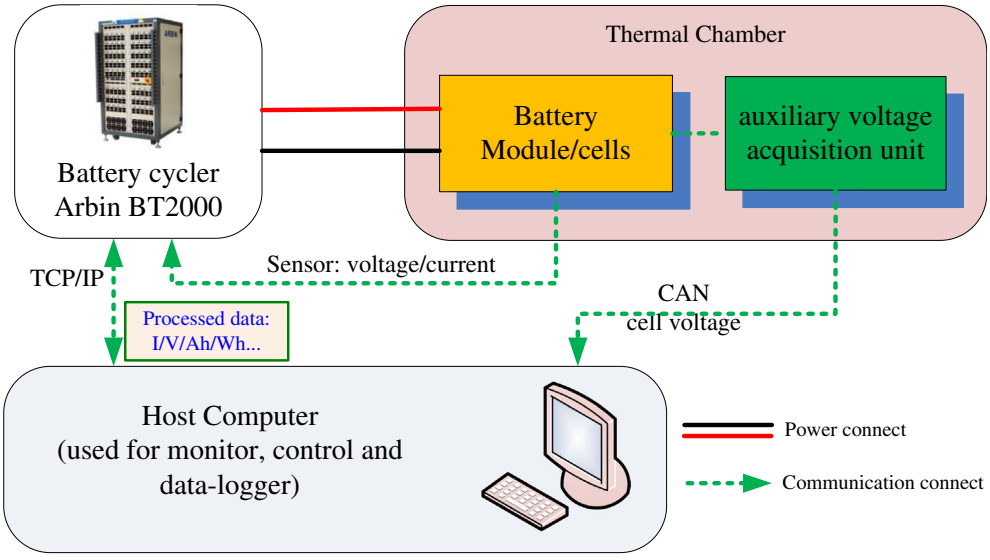

Fig. 10. Configuration of the battery test bench.

is 34.6 Ah and slightly higher than 32 Ah of the nominal capacity. Second, the discharge and charge Coulomb efficiency is conducted. Third, the specific hybrid pulse test has conducted and experiment profiles for cell01 are shown in Fig. 12, where the discharge and charge currents are 0.5C, 1C, 2C and 3C. Noted that the constant current and constant voltage mode is used for charging and discharging the cell in every 10 s pulse and avoiding the cell over-charging or over-discharging, therefore, for a higher SoC, the maximum charging current maybe less than 96 A (3C rate), shown in Fig. 12(c), where the sampling interval Δt is 1 s. Additionally, for the lithium-ion prismatic cell with the nominal capacity of 32 Ah, a discharge current with a 1C rate (32 A) will discharge the full cell capacity in 1 h from fully charged state.

The specific hybrid pulse test is similar with the traditional hybrid pulse power characterization test [27]. The specific hybrid pulse test uses four different charge–discharge currents to improve the applicability of the unit model under a more broad currents operation range of dynamic driving cycles. While the traditional hybrid pulse power characterization test only use 1C (discharge) and 0.75C (charge) currents to build the model, and the model's parameters error will be raised due to the battery's current-dependent relaxation effect and columbic efficiency, etc, are different under higher operating currents.

Another OCV test is carried out to achieve the relationship of SoC vs. OCV and then to identify the parameters of OCV functions in Eq. (3).

In addition to the numerical study using synthetic data, we also conducted the FUDS cycle test to evaluate the prediction precision of the cells classification approach and the unit model with chosen cells. The cycle test is composed of several continuous FUDS cycles, separated by 5 min rest, and SoC operation range is from 90% to 10%. Lastly, we conducted the DST to evaluate the prediction precision of the cells series connected battery pack, where the SoC operation range is from 100% to 20%.

4.2. Parameters identification

For the proposed lumped parameters equivalent circuit model, we need to identify the parameters of OCV functions in Eq. (3). The parameters of K_i ($i = 0, 1, 2, 3, 4, 5$) can be calculated by linear fitting method with the experiment data of the OCV vs. SoC. Then, to identify the other parameters, we firstly have a discretization process for dynamic nonlinear model. We then should build a regression equation for the discretization system. We use a regression equation for the unit model and which is shown in Eq. (20).

$$\begin{cases} U_{t,k} = U_{oc} - U_R - R_P \times I_{p,k} \\ I_{p,k} = \left(1 - \dfrac{\left(1 - \exp\left(\dfrac{-\Delta t}{\tau}\right)\right)}{\left(\dfrac{-\Delta t}{\tau}\right)}\right) \times I_{L,k} + \left(\dfrac{\left(1 - \exp\left(\dfrac{-\Delta t}{\tau}\right)\right)}{\left(\dfrac{-\Delta t}{\tau}\right)} - \exp\left(\dfrac{-\Delta t}{\tau}\right)\right) \times I_{L,k-1} + \exp\left(\dfrac{-\Delta t}{\tau}\right) \times I_{p,k-1} \end{cases} \quad (20)$$

where, $I_{p,k}$ is the outflow current of C_P at the kth sampling intervals, $U_{t,k}$ is the terminal voltage at the kth sampling intervals, $I_{L,k}$ is load current at the kth sampling intervals respectively. The U_{oc} is determined by the SoC–OCV test. The time constant of polarization ($\tau = R_P C_P$) required to be set in advance for regression operation, and for different time constants, different correlation coefficients would be calculated; then an optimum time constant value will be achieved through finding the best correlation coefficient by genetic algorithm [7,14].

4.3. Filtering process

4.3.1. Capacity filtering process

The capacity values for the total of 20 LiPB cells are shown in Table 1. With the 5% of the capacities difference bound, shown in Fig. 13 of the green area (in the web version), we can choose the proper cells.

From Fig. 13, we can find ten cells includes cell02, cell04, cell05, cell08, cell12, cell13, cell14, cell15, cell16 and cell17 are chosen in the first filtering process.

4.3.2. Resistance filtering process

Considering the maximum constant operation current is 5C (160 A), therefore the filtering threshold of the resistance is ± 0.23 mΩ (1% × 3.7 V/160 A), which is round 10% of the cell's resistance. With the parameter identification process for lumped parameter model, we can get the resistance parameters results for the ten cells chosen by capacity filtering process. The results are shown in Fig. 14.

From Fig. 14, we can find nine cells include cell02, cell04, cell05, cell12, cell13, cell14, cell15, cell16 and cell17 are chosen for configuring a series connected battery pack. And we choose the cell02 as the representative cell, thus its model is served as unit model. The parameters identification results for cell02 are shown in Tables 2 and 3. Herein we only list the parameters under the SoC from 60% to 80%.

From Fig. 15, we can find the OCV function is accurate enough for modeling the OCV characteristic of the cell.

5. Verification and discussion

In this section, with the loading profiles test data, the terminal voltage and SoC prediction precision of the unit model is evaluated at first. This is used to verify the reliability of the unit model itself. Then, the estimation accuracy of other cells with the unit model has been verified by the chosen cells or other cells. This is used to verify the expansibility of the unit model when using for other cells. After that, the unit model is used to estimate the terminal voltage and state of the battery packs, and the accuracy of the proposed approach is evaluated at last.

5.1. Cell estimation accuracy

5.1.1. FUDS test data

The FUDS test is a typical dynamic driving cycle, which is often used to evaluate the performance of a vehicle, the effect of control strategies, the SoC estimation algorithms, etc [1,2]. The FUDS test is

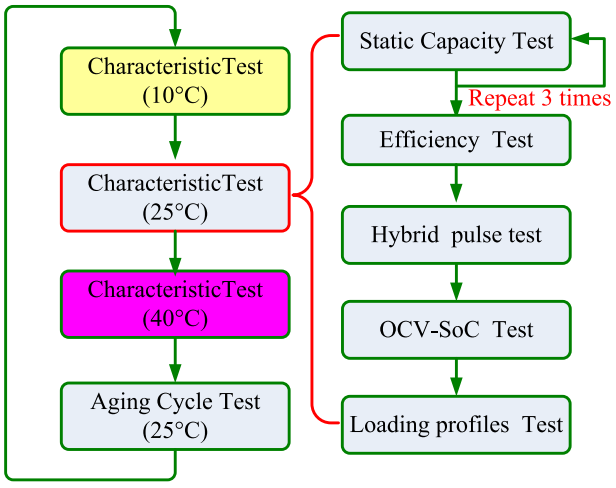

Fig. 11. The battery test schedule.

performed with the current profiles and terminated by a certain amount of Ah removed from the batteries or when the batteries reach a certain voltage level. The experimental current, voltage and calculated SoC profiles of cell02 are shown in Fig. 16. For different cells with different capacities and resistance, the voltage profiles and time length are different.

It is noted that, in all cases, "true" SoC is calculated from the Arbin data-logger using Coulomb counting on measured data. And the "true" SoC is only approximately accurate since current sensor error accumulated over time causes any estimate computed using coulomb counting to eventually divergence. In order to get the reference SoC profiles by an experimental approach. The battery is fully charged to make sure the initial SoC is 100%, such as the accurate SoC initial SoC of DST test is 100%, then it is discharged by nominal current with 10% of its present maximum available capacity, such as the accurate SoC initial SoC of FUDS test is 90%. After the several cycle tests, a further discharge experiment with nominal current is conducted until the battery is fully discharged, and then the true value of the terminal SoC can be calculated according to the definition of SoC. Since the values of the initial SoC and the terminal SoC are accurate, the Coulomb counting method is used to calculate the experimental SoC based on the load current profiles and the Coulomb efficiency map. A proper adjustment coefficient, which is calculated based on the true values of the initial SoC and terminal SoC, is applied during the calculation. The Coulomb counting method with an adjustment approach based on a further discharge experiment can only be used in laboratory, since it is difficult to keep the battery as standing state frequently in practical EVs application.

5.1.2. For chosen cells

Fig. 17 is the estimation results of cell02 with the accurate initial SoC, and the comparative profiles between the estimated terminal voltage and experiment data are shown in Fig. 17(a) and their error profiles are shown in Fig. 17(b). The comparative profiles for SoC are shown in Fig. 17(c) and their error is shown in Fig. 17(d).

Fig. 17(a) and (b) shows the maximum terminal voltage estimation error is less than ±0.03 V (nominal voltage is 3.7 V), Fig. 17(c) and (d) shows the maximum SoC estimation error is less than ±0.5%. Thus, the estimation error for terminal voltage and SoC is less than 1%, which is accurate enough for practical application.

However, an accurate SoC estimation approach depends on two aspects according to the definition of SoC given by Eq. (15), one is the calculation of current integral (ampere-hour counting), and the other is the robustness for initial SoC offset. The above results are only based on the zero initial SoC offset, in order to investigate

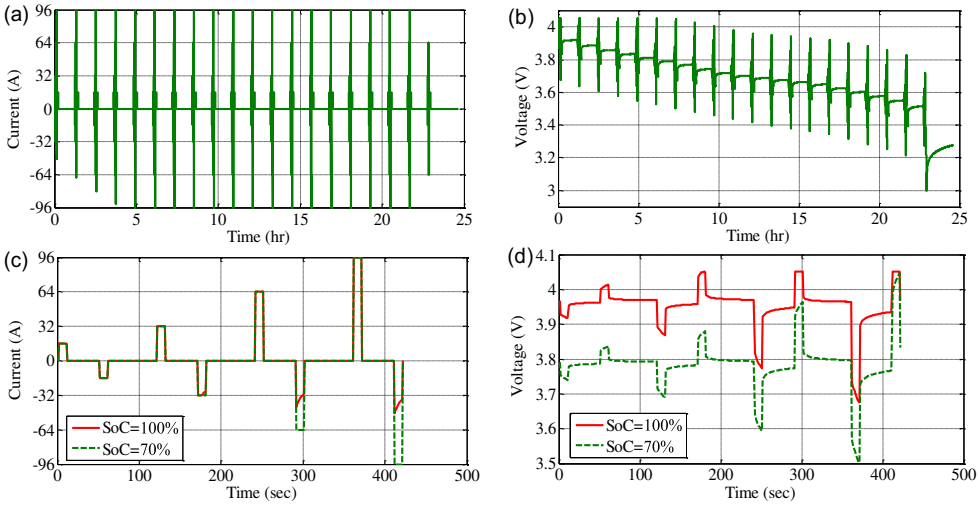

Fig. 12. The specific hybrid pulse test: (a) the current vs. time profiles; (b) the voltage vs. time profiles; the sampling current and voltage profile of under SoC = 100% and 70% shown in (c) and (d).

Table 1
Average available capacities measured by three times (Ah).

Cell01	25.601	Cell02	29.587	Cell03	31.559	Cell04	28.717	Cell05	30.914
Cell06	26.627	Cell07	25.691	Cell08	30.967	Cell09	31.168	Cell10	26.983
Cell11	31.727	Cell12	29.681	Cell13	30.778	Cell14	30.244	Cell15	28.872
Cell16	29.300	Cell17	30.850	Cell18	25.670	Cell19	27.490	Cell20	34.601

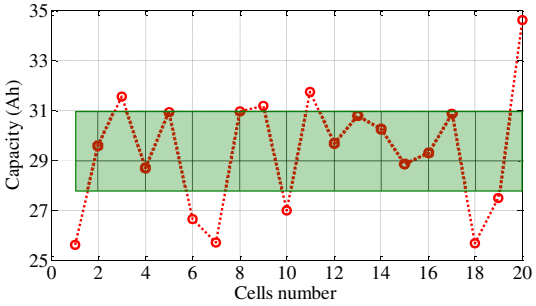

Fig. 13. Capacities of 20 LiPB cells for the first filtering process.

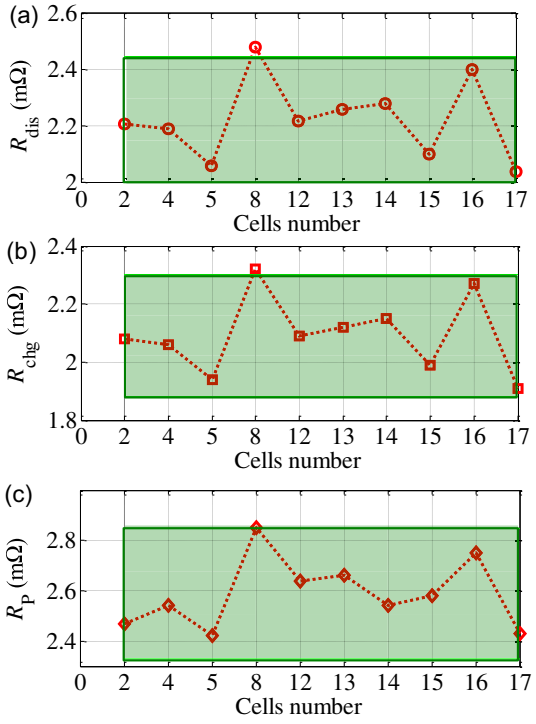

Fig. 14. The second filtering process for the chosen cells in the capacity filtering process.

whether the SoC estimation approach can effectively solve the initial SoC offset, a further simulation analysis is conducted. Two different initial SoC offsets, 30% and 10%, are preset and the corresponding SoC estimations are performed based on the FUDS cycles.

The voltage estimation error profiles are shown in Fig. 18(a), and their zoom figure are shown in Fig. 18(b), the SoC estimation error profiles are shown in Fig. 18(c), and its zoom figure is shown in Fig. 18(d).

It can be found that the AEKF-based approach can accurately estimate the terminal voltage and SoC with different initial SoCs, even with big offset, the convergence value is similar after limited calculated intervals. From Fig. 18(a) and (b), we can find the estimated terminal voltage can trace the reference trajectory accurately and quickly especially with big SoC offset, and the estimated

Table 2
Identification results of OCV function for cell02.

K_0	K_1	K_2	K_3	K_4	K_5
3.641	0.3696	−0.6644	0.6489	1.486e-05	0.06265

Table 3
Identification parameters results of cell02.

SoC/%	C_P/F	R_P/mΩ	R_{dis}/mΩ	R_{chg}/mΩ
60	16,290	2.47	2.21	2.08
65	16,586	2.28	2.19	2.06
70	16,945	2.10	2.17	2.04
75	17,480	1.99	2.15	2.03
80	18,056	1.92	2.13	2.03

trajectory is the same with zero offset after several sampling intervals. From Fig. 18(c), the estimated SoC can trace the reference trajectory accurately and quickly especially with big SoC offset. What's more, from the zoom figure of Fig. 18(d), the SoC estimates can converge to the reference SoC trajectory with several sampling intervals. This is because the proposed approach can precisely estimate the voltage and adjust the Kalman gain according to the terminal voltage error between the measured values and the estimated values timely. The erroneous SoC brings bigger terminal voltage errors, which will in turn causes a big Kalman gain matrix and then compensates the SoC estimation in an efficient closed loop feedback. Thus it can achieve the accurate SoC estimates especially with big SoC offset. Therefore, the proposed data driven-based SoC estimation approach can effectively trace the reference SoC trajectory especially with big SoC offset, and terminal voltage and SoC estimation error in the whole SoC operation ranges are less than 1%. Therefore the unit model is accurate enough to describe the cell's behavior.

Then, to verify the expansibility of the unit model for other cells the AEKF-based method has been replicated 20 times to estimate all terminal voltages and SoCs all the tested cells. Fig. 19 shows the statistic information for the absolute value of the terminal voltage and SoC estimation error of the nine chosen cells.

Fig. 19(a) shows all the maximum terminal voltage errors of the nine cells are less than 51 mV, thus the terminal voltage prediction precision is higher than 98.5%. The mean error and the standard deviation value suggest that most of the error is less than 20 mV. Fig. 19(b) shows all the maximum SoC estimation errors of the nine cells with the same unit model are less than 5%, which meet the design requirement. Therefore, though the proposed filtering method, we can choose the desired cells for battery system, which indicate that the filtering approach is useful.

5.1.3. For other cells

Fig. 20 shows the statistic information for the absolute value of the terminal voltage and SoC estimation error of the rest of the other eleven cells with the unit model.

Fig. 20(a) shows most of the maximum terminal voltage error of the eleven cells is in the ranges of [50 mV, 100 mV], and the mean error and the standard deviation value suggest that the model accuracy is acceptable. Fig. 20(b) shows all the maximum

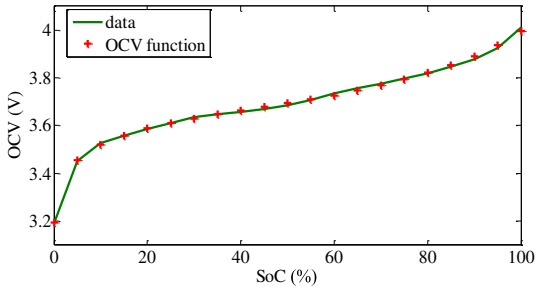

Fig. 15. Comparative curves between the OCV data and function.

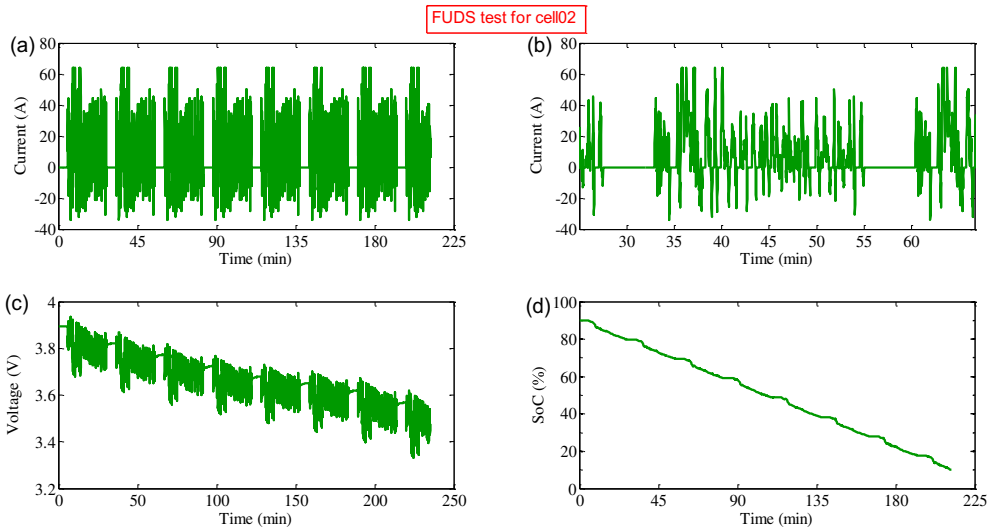

Fig. 16. FUDS experimental profiles of cell02: (a) current; (b) zoom of one current profile (c) voltage; (d) SoC.

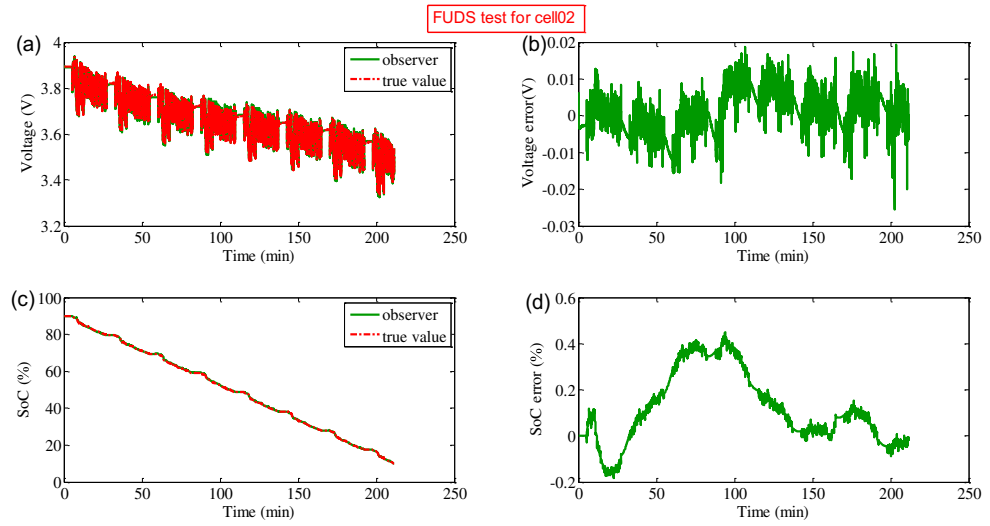

Fig. 17. Estimation results profiles with an accurate initial SoC for cell02: (a) terminal voltage estimation; (b) terminal voltage estimation error; (c) SoC estimation; (d) SoC estimation error.

SoC errors of cell06, cell10, cell11, cell18 and cell19 are less than 5%. Compared with Fig. 19, we can find the filtering approach can ensure that all chosen cells meet the required estimation precision. Therefore the proposed filtering approach is reliable for choosing desirable cells.

5.2. Cells estimation accuracy verification

5.2.1. Dynamic stress test

The DST test is a simple dynamic driving cycle and which is often used to evaluate the SoC estimation algorithms [28]. The DST test is performed with the current profiles and terminated by a certain amount of capacity removed from the batteries or when the batteries reach a certain voltage level. The experimental current, voltage and calculated SoC profiles of chosen cells series connected battery pack are shown in Fig. 21.

5.2.2. Series connected battery pack with the selected LiPB cells

Fig. 22 is the estimation results of battery pack using the unit model with zero SoC offset. The comparative profiles between the estimated terminal voltage and experiment data are shown in Fig. 22(a) and their error is shown in Fig. 22(b). The comparative profiles for SoC are shown in Fig. 22(c) and their error is shown in Fig. 22(d).

Fig. 22(a) and (b) shows the maximum terminal voltage estimation error is less than ±0.5 V, Fig. 22(c) and (d) shows the maximum SoC estimation error is less than ±2%. As a result, both the estimation errors of terminal voltage and SoC of battery pack are less than 2%, and less than the 4.3% of SoC estimation error of cell13. This indicates the estimation error of the pack is not decided by the worst accuracy cell, and the worst cell has been compensated by other cells.

However, an accurate SoC estimation depends on two aspects according the definition of SoC given by Eq. (15), thus a further simulation analysis is conducted. An inaccurate initial SoC, 80%, is preset and the corresponding SoC estimations are performed based on the DST cycles.

The comparative terminal voltage profiles between the estimated profiles with 20% initial SoC offset and the experiment data are shown in Fig. 23(a), and their error profiles are shown in Fig. 23(b), the comparative SoC profiles are shown in Fig. 23(c), and their error profiles are shown in Fig. 23(d).

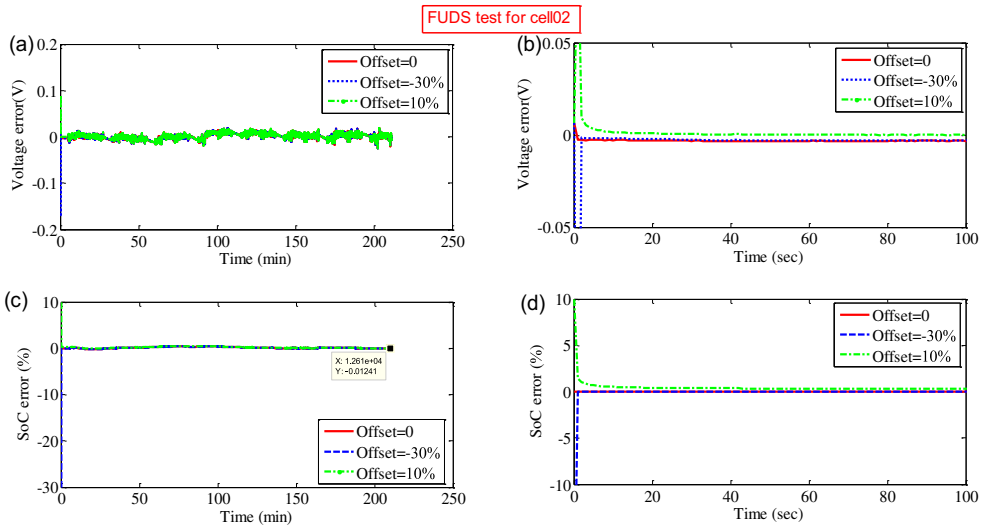

Fig. 18. Estimation results profiles with initial SoC offsets for cell02: (a) terminal voltage estimation; (b) terminal voltage estimation error; (c) SoC estimation error; (d) zoom figure for (c).

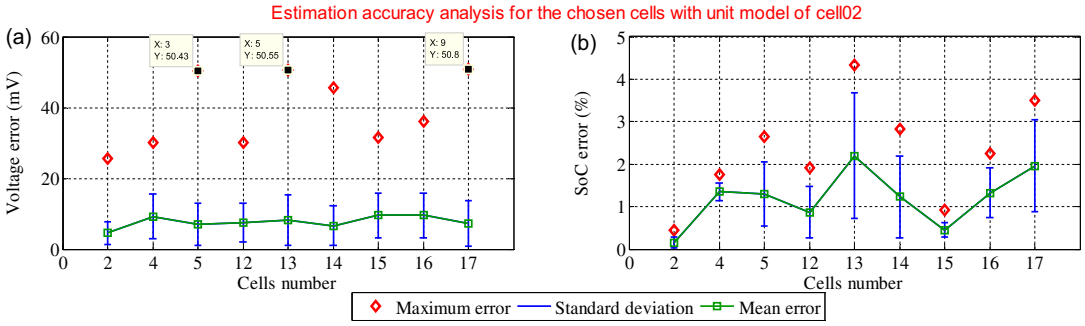

Fig. 19. Estimation accuracy for chosen cells: (a) terminal voltage estimation error; (b) SoC estimation error.

It can be found that the AEKF-based observer accurately estimate the terminal voltage and SoC with different initial SoC, even if with big initial SoC offset, the estimated values converge to reference profiles quickly. From Fig. 23(a) and (b), we can find the terminal voltage estimates can trace the reference trajectory accurately and quickly especially with big offset, and the estimation trajectory is the same with zero SoC offset after several sampling intervals. From Fig. 23(c), the estimated SoC can trace the true trajectory accurately and quickly especially with 20% SoC offset. What's more, from the zoom figure of Fig. 23(d), the SoC estimates can converge to reference SoC trajectory with several sampling intervals. This is because the proposed approach can precisely estimate the voltage and adjust the Kalman gain according to the terminal voltage error between the measured values and the estimated values timely. The erroneous SoC brings bigger terminal voltage errors, which in turn causes a big Kalman gain matrix and then compensate the SoC estimation in an efficient closed loop feedback. Therefore it can get the accurate SoC estimates especially with big SoC offset. Therefore, the proposed data driven-based SoC estimation approach can effectively trace the reference SoC

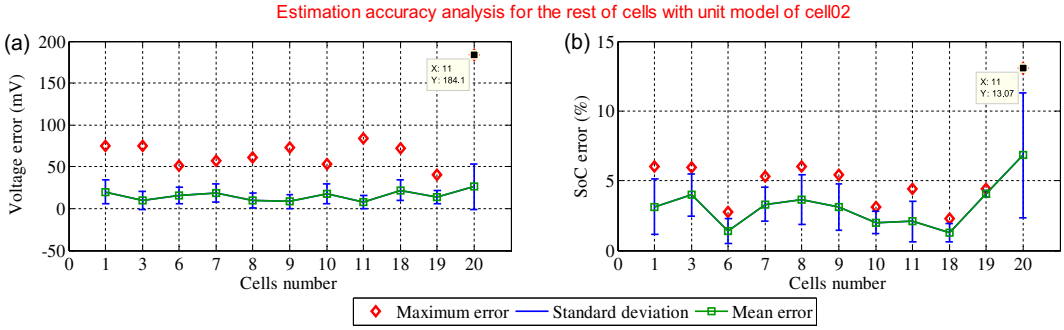

Fig. 20. Estimation accuracy for the rest of cells: (a) terminal voltage estimation error; (b) SoC estimation error.

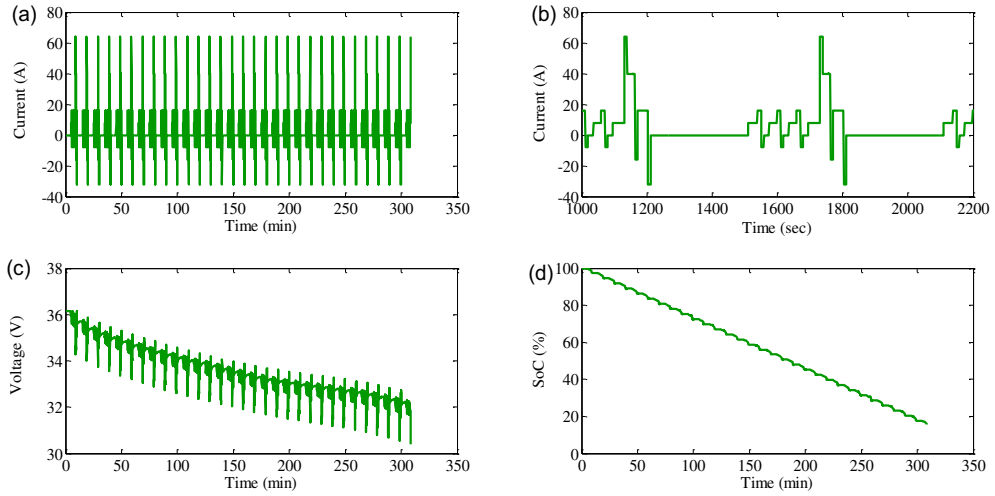

Fig. 21. DST experimental profiles: (a) current; (b) zoom of one current profile (c) voltage; (d) SoC.

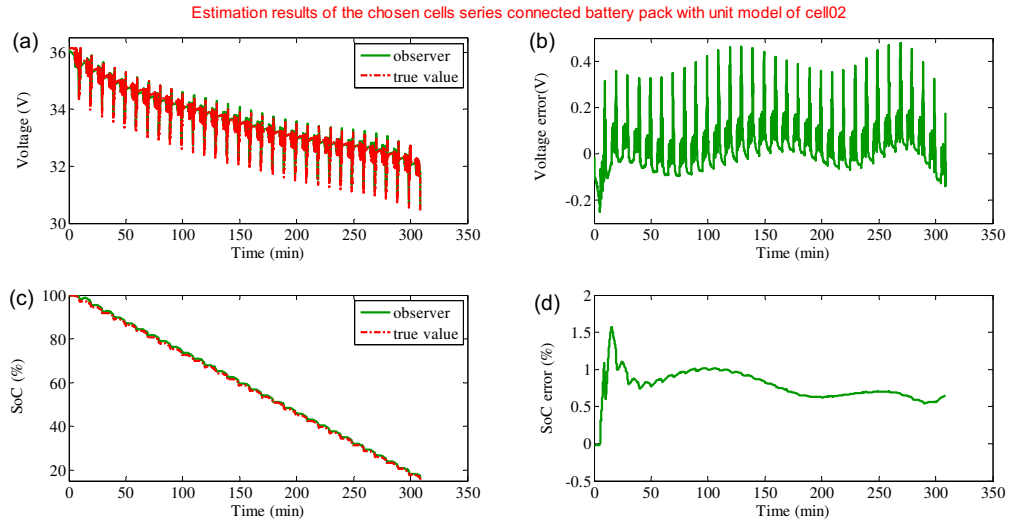

Fig. 22. Estimation result profiles with an accurate initial SoC: (a) terminal voltage estimation; (b) terminal voltage estimation error; (c) SoC estimation; (d) SoC estimation error.

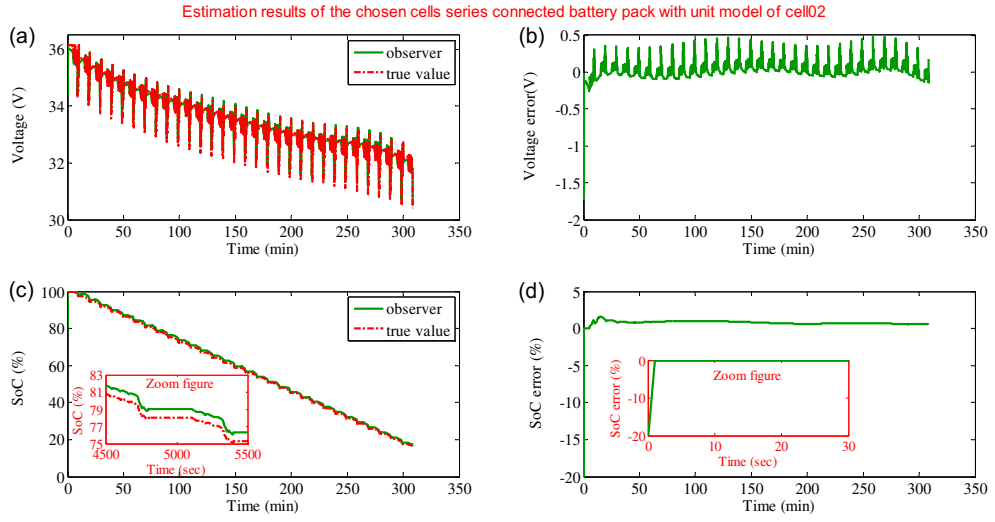

Fig. 23. Estimation result profiles with an inaccurate initial SoC: (a) terminal voltage estimation; (b) terminal voltage estimation error; (c) SoC estimation; (d) SoC estimation error.

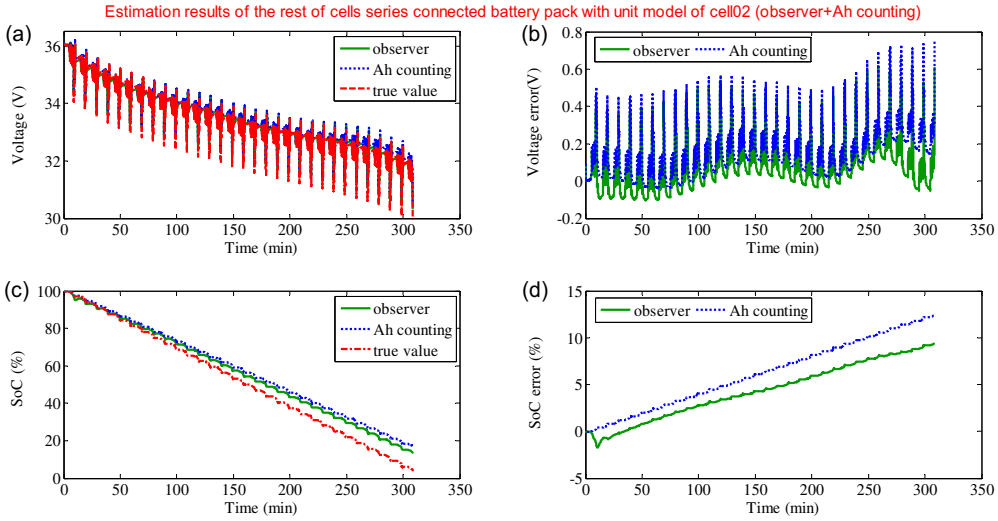

Fig. 24. Estimation result profiles of other pack: (a) terminal voltage estimation; (b) terminal voltage estimation error; (c) SoC estimation; (d) SoC estimation error.

trajectory especially with big SoC offset, and terminal voltage and SoC estimation error in the whole SoC operation ranges are less than 2%. More importantly, with the accurate AEKF-based SoC estimator, the cell-to-cell terminal voltage variance has been compensated, as a result, the total voltage is very close to the ***N*** times terminal voltage of the unit model. Thus the terminal voltage and SoC estimation accuracy is improved and better than the worst cell (cell13), which indicates that the proposed unit model can be efficacious applied to multi-cells series battery pack.

To evaluate the proposed filtering approach and simplified N-cells series connected battery pack model further, we have chosen another nine cells from the rest of eleven cells and two cells (cell01 and cell20) which have worse conformity behavior than others have been eliminated before assembling. The following section discusses the terminal voltage and SoC estimation accuracy for this nine cells series connected battery pack.

5.2.3. Series connected battery pack with rest of the LiPB cells

The comparative terminal voltage profiles among the AEKF-based estimated profiles, Ah counting method-based estimated profiles and the experiment data (true value) are shown in Fig. 24(a), their estimation error is shown in Fig. 24(b), the comparative SoC estimation profiles among the AEKF-based method, Ah counting method and the experiment data (true value) are shown in Fig. 24(c), their estimation error is shown in Fig. 24(d).Where the Ah counting method based SoC estimator is a commonly used method in BMS, herein we want to show the comparative results among the two different SoC estimator with experiment data. In addition to verify the accuracy of the AEKF-based method, we mainly want to verify whether the filtering approach can ensure the estimation accuracy for battery pack.

It can be found that the simplified N-series battery pack model with the unit model estimates the terminal voltage of this battery pack accurately. Specially, with the commonly used Ah counting SoC calculator, the terminal voltage calculation error of battery pack is less than 0.8 V, hence the lumped parameter equivalent circuit model based the unit model is reliable for modeling battery cell and pack with good scalability. Additionally, the terminal voltage prediction precision with AEKF-based SoC estimator is better. From the SoC estimation results of Fig. 24(c) and (d), we can find the AEKF-based SoC estimator has better SoC estimation accuracy than Ah counting method with the accurate initial SoC, and the AEKF-based SoC estimator also can correct the SoC estimation error from the initial SoC offset, however, the Ah counting method based SoC calculator fails.

Based on the above analysis and discussion, the proposed cells filtering approach and the simplified N-cells series connected battery pack model with the unit model is reliable and efficient for cell and pack's modeling and state estimation. It is noted that the used LiPB cells are employed as a case to verify the proposed approach in this paper, thus they do not have good consistency performance in capacity and resistance parameters, therefore, if we use fresh cells to carry out the verification and evaluation, the results may be better and more cells among the tested cells will be chosen.

6. Conclusions

Based on the above analysis, the main concluding remarks can be made below:

(1) To model the dynamic voltage performance of lithium-ion cells accurately, based on our research experience the individually charge and discharge resistor based lumped parameters equivalent circuit model is employed for terminal voltage and state estimation. The electrochemical model is used to build a relationship between the SoC and the open circuit voltage characteristic of the battery. The model not only has the advantages of simulation accuracy for the terminal voltage, but also has a contribution to improve SoC estimation accuracy through an efficient closed-loop feedback. To get accurate model's parameters to improve the dynamic simulation precision, we redefine the hybrid power pulse characteristic test with four different charge–discharge currents.

(2) To avoid or reduce the influence of the drawbacks of cell-to-cell variations in battery packs for electric vehicles application, a cells filtering approach for ensuring the performance of the good capacity/resistance conformity in battery pack has been proposed, which has the potential to achieve voltage/SoC consistency in battery packs, then the ***N*** cells "pack model" can be simplified with a cell lumped parameter equivalent circuit unit model, and its voltage and state behavior can be estimated with the unit model. As a result, the complex, time-consuming and error-prone calibration experiments for each cell in battery system are avoided.

(3) To build an accurate SoC estimation approach for battery packs, an AEKF algorithm-based SoC estimator on the basis of the unit model has been proposed and data driven-based implementation flowchart has been built, which uses the OCV and four other model parameters to build the closed-loop feedback system to adaptive correct the terminal voltage estimation error timely. At last, the terminal voltage and SoC of cells connected battery pack can be achieved.
(4) To analyze the robustness and the reliability of proposed filtering approach and data driven-based SoC estimation approach with the unit model, we have conducted the federal urban driving schedule cycle test. The results indicate the unit model not only ensures higher terminal voltage and SoC estimation accuracy for itself, but also achieves desirable prediction precision for all tested cells, which indicates that the proposed lumped parameter equivalent circuit model has good compatibility and scalability for other cells with similar electrochemical characteristics. Additionally, the result indicates the filtering approach ensures the prediction precision for the chosen cells, the terminal voltage and SoC estimation error are less than 1.5% and 5% respectively.
(5) To analyze the reliability and the prediction precision of proposed filtering approach and simplified equivalent model with the unit model for cells series battery pack, the dynamic stress test has been conducted and the results indicate that the proposed model simulate the terminal voltage and SoC of the battery pack accurately, the pack's estimation error of the chosen cells connected battery pack is less than 2%. However, the pack's estimation error of the series connected battery pack with the rest of cells is much bigger, which suggests the proposed filtering approach for battery pack is useful.

The future work will focus on the SoC and peak power joint estimation approach for the battery pack, and the systematic validation test scheme for available peak power capability estimation.

Acknowledgments

We would like to express our deep gratitude to Professor Chris Chunting Mi in the University of Michigan for many helpful discussions. This work was supported by the National High Technology Research and Development Program of China (2012AA111603, 2011AA11A290) in part, the National Natural Science Foundation of China (51276022) and the Higher school discipline innovation intelligence plan ("111"plan) of China in part, and the Program for New Century Excellent Talents in University (NCET-11-0785) in part.

References

[1] R. Xiong, H. He, F. Sun, K. Zhao, Energies 5 (2012) 1455–1469.
[2] F. Sun, R. Xiong, H. He, W. Li, J.E.E. Aussems, Appl. Energy 96 (2012) 3773–3785.
[3] G.L. Plett, in: EVS24, Stavanger, Norway, May 13–16, 2009.
[4] Y. He, X. Liu, C. Zhang, Z. Chen, Appl. Energy 101 (2013) 808–814.
[5] C. Hu, B.D. Youn, J. Chung, Appl. Energy 92 (2012) 694–704.
[6] H. He, R. Xiong, H. Guo, Appl. Energy 89 (2012) 413–420.
[7] R. Xiong, H. He, F. Suna, X. Liu, Z. Liu, J. Power Sources 229 (2013) 159–169.
[8] V.H. Johnson, J. Power Sources 110 (2002) 321–329.
[9] T. Hansen, C.J. Wang, J. Power Sources 141 (2005) 351–358.
[10] C.C. Chan, E.W.C. Lo, W. Shen, J. Power Sources 87 (2000) 201–204.
[11] W.X. Shen, K.T. Chau, C.C. Chan, Edward W.C. Lo, IEEE Trans. Veh. Technol. 54 (2005) 1705–1712.
[12] H. He, R. Xiong, J. Jilin Univ. (Eng. Technol. Ed.) 41 (2011) 623–628.
[13] G.L. Plett, J. Power Sources 134 (2004) 277–292.
[14] R. Xiong, H. He, F. Sun, K. Zhao, IEEE Trans. Veh. Technol. 62 (2013) 108–117.
[15] J. Hana, D. Kima, M. Sunwoob, J. Power Sources 188 (2009) 606–612.
[16] D. Andre, C. Appel, T. Soczka-Guth, D.U. Sauer, J. Power Sources 224 (2013) 20–27.
[17] J. Kim, J. Shin, C. Chun, IEEE Trans. Power Electron. 27 (2012) 411–424.
[18] E. Karden, S. Buller, R.W. De Doncker, J. Power Sources 85 (2000) 72–78.
[19] Y. Hu, S. Yurkovich, J. Power Sources 198 (2012) 338–350.
[20] H. Dai, X. Wei, Z. Sun, J. Wang, W. Gu, Appl. Energy 95 (2012) 227–237.
[21] Michael A. Roscher, Oliver S. Bohlen, Dirk Uwe Sauer, IEEE Trans. Energy Convers. 26 (2011) 737–743.
[22] Gregory L. Plett, in: EVS24 International Battery, Hybrid and Fuel Cell Electric Vehicle Symposium, 2009.
[23] X. Liu, Y. He, Z. Chen, in: 2010 2nd International Conference on Software Engineering and Data Mining (SEDM), 2010, pp. 27–31.
[24] Y. Zhang, C. Wang, X. Tang, J. Power Sources 196 (2011) 1513–1520.
[25] E. Wood, M. Alexander, T.H. Bradley, J. Power Sources 196 (2011) 5147–5154.
[26] Technical Specification of Battery Management System for Electric Vehicles. Available at: http://www.catarc.org.cn/Upload/file/bzyj/PDF/zhengqiuyijian-sc27-19-bzsm.pdf.
[27] Idaho National Engineering & Environmental Laboratory, Battery Test Manual for Plug-In Hybrid Electric Vehicles, Assistant Secretary for Energy Efficiency and Renewable Energy (EE) Idaho Operations Office, Idaho Falls, ID, USA, 2010.
[28] C. Zhang, J. Jiang, W. Zhang, S.M. Sharkh, Energies 5 (2012) 1098–1115.